Many-body-theory calculation of positronium scattering by atomic hydrogen

Many-body-theory calculation of positronium scattering by atomic hydrogen

A R Swann

School of Mathematics & Physics, Queen's University Belfast, University Road, Belfast BT7 1NN, United Kingdom

E-mail: a.swann@qub.ac.uk

Abstract. The recently developed many-body-theory approach for studying low-energy positronium-atom interactions is applied to calculate positronium scattering by atomic hydrogen. Calculations are carried out for the case where the two electrons are in a spin-triplet state. The elastic scattering phase shifts and cross sections are compared with existing coupled-channel, stochastic-variational, and Kohn-variational results, and excellent agreement is obtained.

1. Introduction

Positronium (Ps) is a light 'atom' consisting of an electron and its antiparticle, the positron. Calculations of Ps scattering by atoms are challenging, since both the target atom and Ps projectile are composite objects. The net electrostatic interaction between the two objects is zero. The presence of the exchange interaction between the target electrons and the electron in Ps results in repulsion for closed-shell targets, since the part of the Ps scattering wave function corresponding to the electron is required to be orthogonal to the occupied target orbitals. Mutual polarization of the target and projectile leads to the long-range attractive van der Waals interaction, which can significantly reduce the effect of the short-range Pauli repulsion [1]. Accurate calculations therefore need to account for the dynamical distortion of both objects during the collision.

A many-body-theory approach to calculating elastic scattering of Ps by closed-shell atoms has recently been developed [2]. The method accounts for virtual excitation of both the Ps and the target in an *ab initio* manner. In Ref. [2], elastic scattering phase shifts and cross sections were calculated for He and Ne targets and found to be in agreement with previous close-coupling [3] and model-potential [1] calculations. The dimensionless pickoff annihilation parameter ${}^1Z_{\rm eff}$ was also calculated for He and Ne and found to be in near-perfect agreement with experimental data [4].

In this work, the many-body-theory method is used to calculate scattering of Ps by atomic hydrogen for Ps momenta $K \leq 1$ a.u. We again consider only the case of elastic scattering, neglecting the possibility of excitation or ionization of the Ps (which is possible for $K \geq \sqrt{3}/2 \approx 0.866$ a.u.). Excitation or ionization of the H atom is only possible for $K \geq \sqrt{3/2} \approx 1.22$ a.u., which is outside the momentum range considered. We also neglect the inelastic process of Ps spin conversion, which is a relativistic effect that is suppressed at low momenta [5].

Unlike the noble-gas targets, the H atom is not closed-shell, and the elastic scattering phase shifts and cross sections depend on the total electron spin, which can have a value of 0 (singlet) or 1 (triplet). Here only the triplet case is considered, since the $1s$ orbital of the H atom is then effectively closed to the additional electron, and the many-body theory can be applied in the usual way.

The paper is structured as follows. In Sec. 2, a description of the salient features of the many-body-theory method for Ps-atom scattering, developed in Ref. [2], is given. The phase shifts and cross section for Ps-H scattering are presented in Sec. 3 and compared with the results of existing accurate *ab initio* calculations. A brief summary and outlook is given in Sec. 4.

Atomic units (a.u.) are used throughout.

2. Theory and numerical implementation

2.1. Many-body theory of electron- and positron-atom interactions

Although conventional treatments of scattering problems are usually based on the Schrödinger equation or Lippman-Schwinger equation, in many-body theory one instead uses the Dyson equation [6]. Before considering the Ps scattering problem, we first solve the Dyson equation for an electron interacting with the target atom and the Dyson equation for a positron interacting with the target atom. These equations are given by

$$(H_0^{\pm} + \Sigma_\varepsilon^{\pm})\psi_\varepsilon^{\pm}(\mathbf{r}) = \varepsilon\psi_\varepsilon^{\pm}(\mathbf{r}). \tag{1}$$

Here, $H_0^{\pm}$ is the zeroth-order Hamiltonian, e.g., that of the electron ($-$) or positron ($+$) in the field of the atom, described in the Hartree-Fock approximation, and ε and $\psi_\varepsilon^{\pm}$ are the energy and quasiparticle wave function, respectively. The operator $\Sigma_\varepsilon^{\pm}$ is the nonlocal, energy-dependent, many-body correlation potential, which is equal to the electron or positron self-energy in the field of the atom; it acts on $\psi_\varepsilon^{\pm}$ as an integral operator, viz.,

$$\Sigma_\varepsilon^{\pm}\psi_\varepsilon^{\pm}(\mathbf{r}) \equiv \int \Sigma_\varepsilon^{\pm}(\mathbf{r},\mathbf{r}')\psi_\varepsilon^{\pm}(\mathbf{r}')\, d^3\mathbf{r}'. \tag{2}$$

As a result of the spherical symmetry of the problem, (1) can be solved separately for each electron or positron orbital angular momentum l, with the wave function in the form

$$\psi_\varepsilon^{\pm}(\mathbf{r}) = \frac{1}{r}\chi_{\varepsilon l}^{\pm}(r)Y_{lm}(\Omega), \tag{3}$$

where Y_{lm} is a spherical harmonic, m is the magnetic quantum number, Ω denotes solid angle, and $\chi_{\varepsilon l}^{\pm}$ is a radial function to be determined. Rather than working with the self-energy operator $\Sigma_\varepsilon^{\pm}$ in coordinate space, it is usually more convenient to work with its matrix elements in the basis of eigenstates $\varphi_\varepsilon^{\pm}$ of the Hartree-Fock Hamiltonian $H_0^{\pm}$. We have

$$\langle\varepsilon'|\Sigma_E^{\pm}|\varepsilon\rangle = \int_0^\infty\int_0^\infty P_{\varepsilon' l}^{\pm}(r')\Sigma_{El}^{\pm}(r,r')P_{\varepsilon l}^{\pm}(r)\, dr\, dr', \tag{4}$$

where $H_0^{\pm}\varphi_\varepsilon^{\pm} = \varepsilon\varphi_\varepsilon^{\pm}$, $\varphi_\varepsilon^{\pm}(\mathbf{r}) = r^{-1}P_{\varepsilon l}^{\pm}(r)Y_{lm}(\Omega)$, and $\Sigma_{El}^{\pm}$ is the self-energy for partial wave l.

The matrix elements $\langle\varepsilon'|\Sigma_E^{\pm}|\varepsilon\rangle$ are calculated using the diagrammatic technique [6]. Figure 1 shows the main contributions to the electron and positron self-energy. The first diagram for both the electron (top row) and positron (bottom row) accounts for the attractive long-range polarization potential $-\alpha/2r^4$, where α is the dipole polarizability of the atom. The remaining diagrams only contribute at short range. The second diagram for the positron represents the important process of virtual Ps formation, with the hatched Γ block denoting an infinite series of electron-positron Coulomb interactions [7, 8]. The electron and positron self-energy matrix

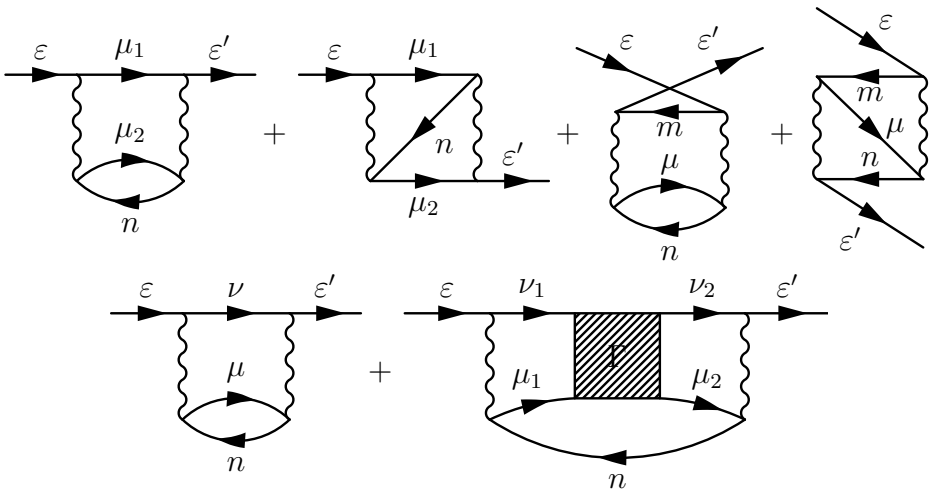

Figure 1. The main contributions to the self-energy of the electron (top row) and positron (bottom row) in the field of the atom. Lines labelled ε or ε' represent electron or positron Hartree-Fock wave functions. Lines labelled ν, ν_1, and ν_2 (μ, μ_1, and μ_2) represent positron (excited electron) states, which are summed over. Lines labelled m and n represent holes in the atomic ground state. Wavy lines represent Coulomb interactions. The shaded Γ block represents the sum of the electron-positron ladder-diagram series [7, 8], which accounts for virtual Ps formation.

elements are calculated as described in Ref. [8], using a B-spline basis with 40 splines of order 6, defined over an exponential knot sequence, in a spherical cavity of radius 30 a.u.

In Ref. [2], it was found that the electron and positron self-energy matrix elements $\langle\varepsilon'|\Sigma_E^{\pm}|\varepsilon\rangle$ depend rather weakly on the energy E at which they are calculated. Consequently, all calculations for the He and Ne targets were carried out for a fixed energy of $E = 0$ [2]. In the present calculations for the H target, the matrix elements $\langle\varepsilon'|\Sigma_E^{\pm}|\varepsilon\rangle$ are again calculated for a fixed energy of $E = 0$.

After the self-energy matrix elements have been calculated, (1) is solved to obtain the energy eigenvalues ε and wave functions $\psi_\varepsilon^{\pm}$ in the spherical cavity. For the electron, there are negative-energy states, which correspond to holes in the atomic ground state, along with positive-energy excited pseudostates that span the continuum. For the positron, there are only positive-energy 'continuum' pseudostates.

2.2. Many-body theory of Ps-atom interactions

The wave function Ψ of Ps satisfies the two-particle Dyson equation

$$\left(H_0^- + \Sigma_E^- + H_0^+ + \Sigma_E^+ + V + \delta V_E\right)\Psi = \mathcal{E}\Psi, \tag{5}$$

where V is the electron-positron Coulomb interaction, and δV_E is the energy-dependent screening correction that arises from polarization of the atom. As with the electron and positron self-energy, we calculate matrix elements of δV_E at a fixed energy of $E = 0$. Figure 2 shows the diagrammatic representation of the matrix elements of V and δV_E. Diagram (a) is the bare Coulomb interaction V. Diagram (b) is the main contribution to δV_E; it cancels the long-range electron and positron r^{-4} polarization potentials and results in the asymptotic R^{-6} van der Waals potential, where R is the distance from the Ps centre of mass to the atom. The exchange diagrams (c) and (d) are typically much smaller and partially cancel each other, so they can be neglected.

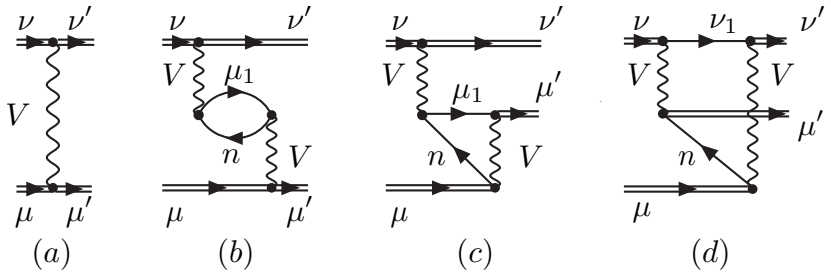

Figure 2. The main contributions to the electron-positron interaction in Ps: (a) the bare Coulomb interaction V; (b)–(d), screening δV_E with exchange contributions (with mirror images). Double lines labeled ν (μ) represent positron (electron) Dyson states in the field of the atom.

A Ps wave function with angular momentum J and parity Π can be constructed from the single-particle electron and positron Dyson states $\psi^{\pm}_{\varepsilon}$ as [1, 9]

$$\Psi_{J\Pi}(\mathbf{r}_-, \mathbf{r}_+) = \sum_{\mu,\nu} C^{J\Pi}_{\mu\nu} \psi^-_\mu(\mathbf{r}_-)\psi^+_\nu(\mathbf{r}_+), \tag{6}$$

where only products of electron and positron states whose orbital angular momenta satisfy $|l_\mu - l_\nu| \leq J \leq l_\mu + l_\nu$ and $(-1)^{l_\mu + l_\nu} = \Pi$ are included in the expansion. To ensure orthogonality of the electron part of the Ps wave function to the occupied target orbitals, the negative-energy electron states are excluded from the expansion. The energy eigenvalues $\mathcal{E}$ and expansion coefficients $C^{J\Pi}_{\mu\nu}$ are found by solving the matrix eigenvalue problem for the Hamiltonian matrix

$$\langle \nu'\mu'|H|\mu\nu\rangle = (\varepsilon_\mu + \varepsilon_\nu)\delta_{\mu\mu'}\delta_{\nu\nu'} + \langle \nu'\mu'|V + \delta V_E|\mu\nu\rangle, \tag{7}$$

where ε_μ and ε_ν are the energies of the Dyson states ψ^-_μ and ψ^+_ν, respectively. We carry out calculations for $J^\Pi = 0^+$, 1^-, and 2^+ to investigate S-, P-, and D-wave scattering of Ps($1s$), respectively. To ensure the accurate description of Ps states by (6), we confine the constituent electron and positron of the Ps to a cavity of radius $R_c = 10$–16 a.u. [1, 9]. The reason for using a smaller cavity here than when calculating the self-energy matrix elements for the electron and positron is to assist convergence of the expansion (6) with respect to the maximum orbital angular momentum of the states included: if the electron-positron pair were allowed to move far away from the centre of the cavity, then the solid angle subtended by the electron-positron pair would be small, and electron and positron states with large orbital angular momenta would need to be included in (6) to accurately resolve the internal structure of Ps. To accurately represent the positive-energy 'continuum' in the cavity, we use a second B-spline basis of 60 splines of order 9, defined over a quadratic-linear knot sequence [1]. Calculations are performed with a range of different numbers of radial states and orbital angular momenta included in (6), up to $n_{\max} = 20$ and $l_{\max} = 20$ and extrapolated to $n_{\max} \to \infty$ and $l_{\max} \to \infty$ [9]. The inclusion of such high angular momenta in the expansion of the Ps wave function is necessary to ensure convergence of the single-centre expansion about the target nucleus.

The elastic scattering phase shifts η_L ($L = 0$, 1, 2) are obtained from the discrete Ps($1s$) energy eigenvalues in the cavity as [1]

$$\eta_L = \tan^{-1} \frac{J_{L+1/2}(K[R_c - \rho])}{Y_{L+1/2}(K[R_c - \rho])} \pmod{\pi}, \tag{8}$$

where K is the Ps centre-of-mass momentum (which is related to the Ps energy eigenvalue by $\mathcal{E} = -1/4 + K^2/4$), J_α and Y_α are the Bessel and Neumann functions, respectively, and ρ is

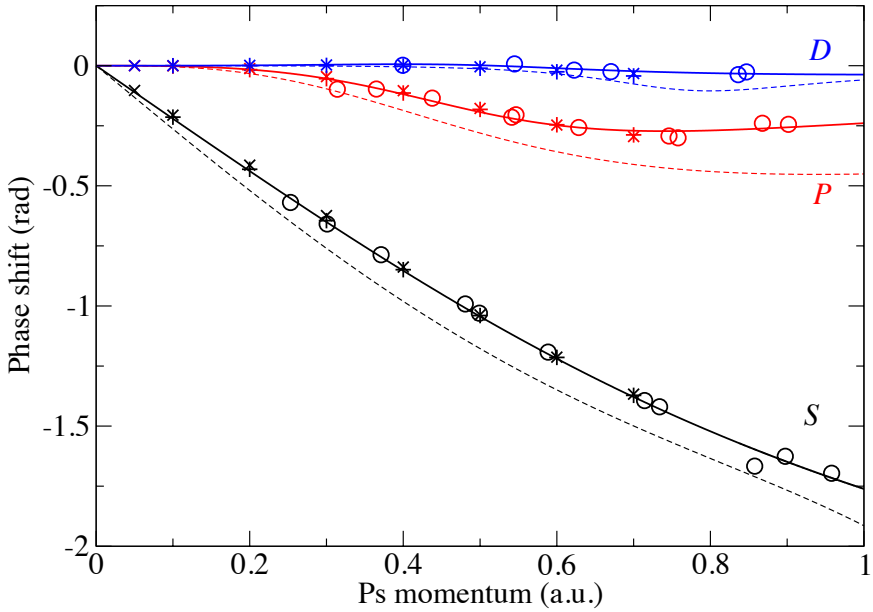

Figure 3. Phase shifts for elastic scattering of Ps by H, with the two electrons in the spin triplet state. Circles, phase shifts calculated at discrete value of the Ps centre-of-mass momentum; solid curves, effective-range-theory fits to the phase shifts; crosses, coupled-channel calculations [10]; plusses, Kohn-variational calculations [11]. The dashed curves are the corresponding frozen-target phase shifts, obtained by setting $\Sigma_E^{\pm} = 0$ and $\delta V_E = 0$. Black, red, and blue symbols and curves are for the S, P, and D waves, respectively.

the collisional radius of Ps at the wall of the cavity [1, 9]. Effective-range-theory fits are used to interpolate the phase shifts calculated at the discrete values of the Ps centre-of-mass momentum. The elastic cross section σ is then obtained as

$$\sigma = \frac{4\pi}{K^2} \sum_L (2L+1) \sin^2 \eta_L. \tag{9}$$

3. Results for elastic Ps-H scattering

The S-, P-, and D-wave phase shifts for elastic scattering of Ps on H, with the two electrons in the spin-triplet state, are shown in figure 3. The S-wave phase shift is a negative and decreasing function of K for low K, which indicates that the scattering length is positive and the effective Ps-H interaction is repulsive. This is similar to the picture of low-energy Ps scattering from He and Ne [2].

Also shown in figure 3 are coupled-channel calculations of Blackwood *et al.* [10], which included 14 Ps and 14 H states in the expansion of the wave function for the S wave, and 9 Ps and 9 H states for the P and D waves. Additionally, complex-Kohn-variational calculations of Woods *et al.* [11] are shown. We see that there is excellent agreement between the present calculations and those of Blackwood *et al.* [10] and Woods *et al.* [11] for all three partial waves.

A frozen-target calculation of the phase shifts, where distortion of the Ps is accounted for but the H atom is kept in its ground state, can be carried out by setting $\Sigma_E^{\pm} = 0$ and $\delta V_E = 0$ in (1) and (6). The results of such a calculation are also shown in figure 3. These phase shifts are lower (i.e., more negative) than the many-body-theory phase shifts. This is as expected: the removal of the attractive correlation effects, which at long range give rise to the attractive van der Waals interaction, leads to the Ps-H interaction becoming even more repulsive.

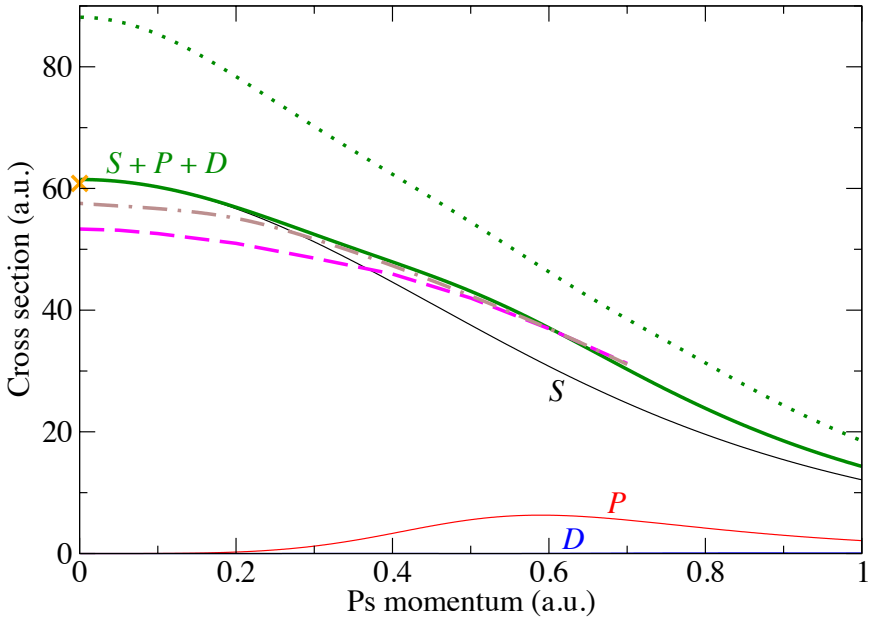

Figure 4. Cross section for elastic scattering of Ps by H, with the two electrons in the spin-triplet state. Solid black curve, S-wave contribution; solid red curve, P-wave contribution; solid blue curve (barely visible), D-wave contribution; thick solid green curve, total. Dashed magenta curve, coupled-channel calculation [10]; dot-dashed brown curve, Kohn-variational calculation [11]; orange cross, stochastic-variational calculation [12]. The dotted green curve is the frozen-target calculation, obtained by setting $\Sigma_E^{\pm} = 0$ and $\delta V_E = 0$.

The elastic scattering cross section is shown in figure 4. Also shown are the corresponding frozen-target result, the coupled-channel calculation of Blackwood *et al.* [10], the Kohn-variational calculation of Woods *et al.* [11], and the zero-energy result of a stochastic-variational calculation [12]. The scattering is almost purely due to the S wave for momenta up to $K \approx 0.2$ a.u., after which the P-wave partial cross section becomes visible. The D wave barely contributes in the momentum range considered, and consequently, the cross section is converged across the momentum range considered with respect to the number of partial waves L included in (9).

The frozen-target value of the cross section at zero momentum is 40% larger than the many-body-theory value, which emphasizes the need to account for distortion of the target to obtain accurate results. The many-body-theory value at zero momentum is in very close agreement with the stochastic-variational result [12]; indeed, the many-body-theory value of the scattering length is 2.21 a.u., while the stochastic-variational value is 2.2 a.u.

At low momenta, the many-body-theory cross section is slightly larger than the coupled-channel [10] and Kohn-variational [11] calculations, which gave values of 2.06 a.u. and 2.14 a.u., respectively, for the scattering length. However, the present cross section comes into very close agreement with the coupled-channel [10] and Kohn-variational [11] calculations at momenta $K \approx 0.5$ a.u. and $K \approx 0.3$ a.u., respectively.

4. Conclusions

Many-body theory has been used to investigate elastic scattering of Ps by atomic hydrogen, for the case where the two electrons have the total spin of 1. The scattering phase shifts, cross section, and scattering length have been calculated and compared with existing *ab initio* calculations,

with excellent overall agreement being achieved.

Although the many-body-theory approach to Ps-atom scattering had previously been successfully applied to the many-electron He and Ne targets [2], carrying out calculations for H provides a useful verification of the reliability of the results obtained, as for H there are highly accurate calculations in the literature with which to compare. The main source of uncertainty in the many-body-theory calculations stems from the single-centre expansion of the Ps wave function in terms of single-particle electron and positron wave functions. It is vital to ensure that sufficiently many radial states and angular momenta are included in the expansion to enable robust extrapolation of the Ps energies to the limits $n_{\max} \to \infty$ and $l_{\max} \to \infty$. Some further uncertainty arises from the dependence of $\Sigma_E^{\pm}$ and δV_E on energy, the neglect of higher-order contributions to $\Sigma_E^{\pm}$ and δV_E, and using effective-range theory to extrapolate the S-wave phase shift to the limit $K \to 0$ (which determines the value of the scattering length and zero-energy cross section). However, the excellent agreement of the present scattering length with the stochastic-variational [12] and Kohn-variational [11] values and the very good agreement of the cross section at higher momenta with the Kohn-variational [11] and coupled-channel [10] calculations gives confidence in the many-body-theory approach and its application to other targets.

Future work will entail calculating elastic Ps scattering on heavier noble-gas atoms, viz., Ar, Kr, and Xe, for which the best existing *ab initio* calculations are of the frozen-target type [1, 13, 14]. Preliminary calculations indicate that, as has been found for H, He, and Ne, the net Ps-atom interaction for these targets is repulsive at low Ps energies; this is in contrast to the results of recent experiments which predicted the low-energy Ps-atom interaction to be attractive for Ar and Xe [15]. For these targets, the pickoff annihilation parameter $^1Z_{\rm eff}$ can also be calculated, which should help resolve the uncertainty in the experimental measurements of this quantity for Kr and Xe due to the contribution of spin-orbit quenching to the total annihilation rate [4, 16].

Acknowledgments

I am grateful to D V Fursa for fruitful conversations at ICPEAC 2019 in Deauville and to G F Gribakin for helpful comments on the manuscript. This work was supported by the Department for Employment and Learning, Northern Ireland, UK, and by the EPSRC UK, Grant No. EP/R006431/1.

References

[1] Swann A R and Gribakin G F 2018 *Phys. Rev.* A **97** 012706
[2] Green D G, Swann A R and Gribakin G F 2018 *Phys. Rev. Lett.* **120** 183402
[3] Walters H, Yu A, Sahoo S and Gilmore S 2004 *Nucl. Instrum. Methods Phys. Res.* B **221** 149
[4] Charlton M 1985 *Rep. Prog. Phys.* **48** 737
[5] Mitroy J and Novikov S A 2003 *Phys. Rev. Lett.* **90** 183202
[6] Fetter A L and Walecka J D 2003 *Quantum Theory of Many-Particle Systems* (New York: Dover)
[7] Gribakin G F and Ludlow J 2004 *Phys. Rev.* A **70** 032720
[8] Green D G, Ludlow J A and Gribakin G F 2014 *Phys. Rev.* A **90** 032712
[9] Brown R, Prigent Q, Swann A R and Gribakin G F 2017 *Phys. Rev.* A **95** 032705
[10] Blackwood J E, McAlinden M T and Walters H R J 2002 *Phys. Rev.* A **65** 032517
[11] Woods D, Ward S J and Van Reeth P 2015 *Phys. Rev.* A **92** 022713
[12] Ivanov I A, Mitroy J and Varga K 2001 *Phys. Rev. Lett.* **87** 063201
[13] Blackwood J E, McAlinden M T and Walters H R J 2002 *J. Phys.* B **35** 2661
[14] Blackwood J E, McAlinden M T and Walters H R J 2003 *J. Phys.* B **36** 797
[15] Brawley S J, Fayer S E, Shipman M and Laricchia G 2015 *Phys. Rev. Lett.* **115** 223201
[16] Saito H and Hyodo T 2006 *Phys. Rev. Lett.* **97** 253402